

Clinical-Prostate cancer
Free-indocyanine green-guided pelvic lymph node dissection during
radical prostatectomy

Francesco Claps, M.D.^{a,b,*}, Pedro de Pablos-Rodríguez, M.D.^{a,c}, Álvaro Gómez-Ferrer, M.D.^a,
Juan Manuel Mascarós^a, Josè Marenco, M.D.^a, Argimiro Collado Serra, M.D.^a,
Juan Casanova Ramón-Borja, M.D.^a, Ana Calatrava Fons, M.D.^d, Carlo Trombetta, M.D.^b,
Jose Rubio-Briones, M.D. Ph.D.^a, Miguel Ramírez-Backhaus, M.D. Ph.D.^a

^a Department of Urology, Valencian Oncology Institute Foundation, FIVO, Valencia Spain

^b Urological Clinic, Department of Medicine, Surgery, and Health Sciences, University of Trieste, Trieste Italy

^c Research Institute of Biomedical and Health Sciences, Doctoral School of University of Las Palmas de Gran Canaria Spain

^d Department of Pathology, Valencian Oncology Institute Foundation, FIVO, Valencia Spain

Received 26 February 2022; received in revised form 8 June 2022; accepted 7 August 2022

Abstract

Introduction and objectives: Extended Pelvic Lymph Node Dissection (ePLND) remains the most accurate technique for the detection of occult lymph node metastases (LNMs) in prostate cancer (CaP) patients. Here we aim to examine whether free-Indocyanine Green (F-ICG) could accurately assess the pathological nodal (pN) status in CaP patients during real-time lymphangiography as a potential replacement for ePLND.

Materials and methods: 219 consecutive patients undergoing F-ICG-guided PLND, ePLND and radical prostatectomy (RP) for clinical-localized CaP were included in this prospective single-center study. The pathological outcomes of F-ICG-guided PLND were compared to confirmatory ePLND. Parameters of a binary diagnostic test for the proper classification of the pN status of patients ('per-patient' analysis) and for the probability of detecting all the metastatic LNMs ('per-node' analysis) were calculated. Outcome measures were prevalence, accuracy (Acc), sensitivity (Se), negative predictive value (NPV), and likelihood ratio of a negative F-ICG-guided PLND test result [LR(−)].

Results: F-ICG-guided PLND successfully visualized LNMs in all procedures with no adverse events. The overall per-patient F-ICG staging Acc was 97.7%, Se was 91.4%, with a NPV of 97.0%, and LR(−) of 8.6%. At the overall per-node level, 4,780 LNMs were removed and 1,535 (32.1%) were fluorescent in vivo. F-ICG-guided PLND identified LNMs with a Se of 63.4%.

Conclusions: This study confirms that F-ICG-guided lymphangiography correctly staged almost 98% of patients. The high per-patient NPV suggested that avoiding ePLND is safe for most patients when F-ICG stained nodes were pN0. Thus, more conservative approaches might minimise perioperative morbidity during LNMs diagnosis in selected patients. © 2022 Elsevier Inc. All rights reserved.

Keywords: Prostate cancer; Extended pelvic lymph node dissection; Sentinel lymph node biopsy; Indocyanine green; Fluorescence

1. Introduction

Prostate cancer (CaP) is the most frequent urological malignancy and the fifth leading cause of cancer deaths

Awarded at the American Urological Association (AUA) Meeting 2020 with the "Best Poster" prize at dedicated Session of the Meeting "Prostate Cancer: Localized: Surgical Therapy".

Funding: This research did not receive any specific grant from funding agencies in the public, commercial, or not-for-profit sectors.

*Corresponding author: Tel/: +39 3408572026.

E-mail address: claps.francesco@gmail.com (F. Claps).

among men worldwide [1]. Approximately half of these patients have intermediate or high-risk organ-confined disease and up to 30% harbor lymph node metastases (LNMs) [2].

Several nomograms that incorporate clinical, pathological and imaging parameters are available to computationally estimate the probability of LNMs a given patient has [2–4]. However, extended pelvic lymph node dissection (ePLND) remains the most accurate staging procedure to assess LN status [5,6]. Nonetheless ePLND was found to improve staging accuracy but survival advantage

remained controversial [7]. Moreover, meticulous ePLND is time-consuming, surgeon-dependent, and implies an increased risk of patient morbidity [7].

Personalised lymphatic mapping procedures such as sentinel node (SN) biopsy techniques have been described in CaP patients in order to target LN dissection without decreasing diagnostic accuracy [8]. Similarly, the use of free-indocyanine green (F-ICG) [9], alone or in combination with other radiotracers [10], has also shown promising results via lymphangiography [9,11,12]. ICG is a nontoxic, nonradioactive compound which fluoresces when stimulated by near-infrared (NIR) light [13,14].

In this current study we tested the hypothesis that transperineal injection of diluted F-ICG would enable real-time NIR lymphangiography. Our primary objective was to evaluate the ability of F-ICG to stage the LN-status of patients who underwent laparoscopic radical prostatectomy (RP). Thus, we explored the role of F-ICG-guided PLND as a potential replacement for ePLND. To this end, pathological outcomes of selective F-ICG-guided PLND were evaluated and compared with ePLND as the current standard-of-care.

2. Materials and methods

2.1. Patients and setting

From January 2014 to December 2018, 219 consecutive patients with CaP who had been scheduled for a laparoscopic RP were recruited to this study. This prospective study was completed in accordance with the principles of the Declaration of Helsinki and was approved by the ethics committee (Institutional Review Board approval CaPROS-IVO) at the Valencian Oncology Institute Foundation. According to the EAU risk groups criteria [15], all the patients included had an intermediate- or high-risk of biochemical recurrence clinical-localized CaP and underwent laparoscopic F-ICG-guided PLND plus ePLND and RP. Three experienced surgeons performed the surgical procedures and clinical, surgical, and pathological data were prospectively collected and analyzed.

2.2. Surgical procedure and pathological examination

The surgical techniques used for ICG administration, fluorescent PLND, and subsequent ePLND have been previously described [11,16]. F-ICG was already available at our Institute for Vascular Surgery purposes. A dose of 25 mg F-ICG was diluted in 5 ml sterile water solution and was used for transperineal injection in the middle of the transitional zone of each prostatic lobe. Surgery started with F-ICG-guided PLND. ICG stained LNs were independently removed, and separately labelled. Only fluorescent LNs inside the small pelvis (internal, external, and common iliac, obturator, and presacral regions) were considered. Regular ePLND followed the F-ICG-guided PLND.

Extended template was defined as the region encompassed by the ureteric crossing and including the bifurcation of the common iliac artery, along the external iliac down to the circumflex iliac vessels until the Cloquet's node, internal iliac vessels and obturator fossa. Umbilical artery was individualized from the iliac vessels, and the medial lymphatic tissue was sent together with the internal iliac specimen. The presacral region was defined as the triangular area between the medial borders of the common iliac arteries. Finally, RP was performed on a standard fashion. A dedicated laparoscopic fluorescence imaging system was used (D-lightP, Karl Storz). All available tissue from ICG stained LNs was sliced at 250 μm by a single dedicated uro-pathologist. The rest of nodes from ePLND were processed in the standard manner.

2.3. Statistical analysis

Statistical analyses as well reporting and interpretation of the results were conducted according to established guidelines [17]. Descriptive analysis included frequencies and proportions for categorical variables. Medians and interquartile range (IQR) were reported for continuous variables. The Mann-Whitney-U test or Kruskal-Wallis were used for comparison of the continuous data and the Chi-square or Fisher's exact test for categorical data. Results were stratified according to the EAU clinical-risk-classification criteria [15] and all tests were 2-sided with a level of significance set at $P < 0.05$. We calculated the prevalence, accuracy (Acc), sensitivity (Se), negative predictive value (NPV), and likelihood ratio of a negative F-ICG-guided PLND test result [LR(-)] with 95% Confidence Intervals (CI) for the proper classification of the pathological nodal (pN) status of our patients ('per-patient' analysis, as shown in Fig. 1). We also calculated the prevalence, Acc, Se, and LR(-) with 95%CI of retrieving all the metastatic LNs ('per-node' analysis). The statistical analyses were performed with RStudio, v.1.2.1335.

3. Results

3.1. Preoperative demographic and disease characteristics

The clinical and demographic characteristics of the 219 patients included are provided in Table 1. Median age at surgery was 64 years (IQR 59–69) and 149 (68.0%) patients had intermediate-risk disease. Median prostate-specific antigen (PSA) was 6.8 ng/ml (IQR 5–9) and 34 (15.5%) patients presented with locally-advanced disease ($\geq\text{T3}$), 29 (13.2%) of which had a Gleason score was ≥ 8 .

3.2. Pathological and surgical outcomes

Table 1 provides detailed descriptive and pathological outcomes data for the study cohort. Median operative time was 275 minutes (range 240–300). Fluorescent lymphatic

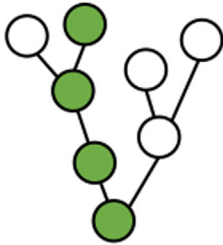
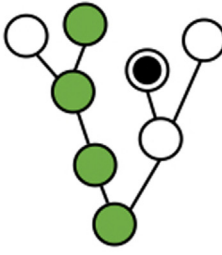
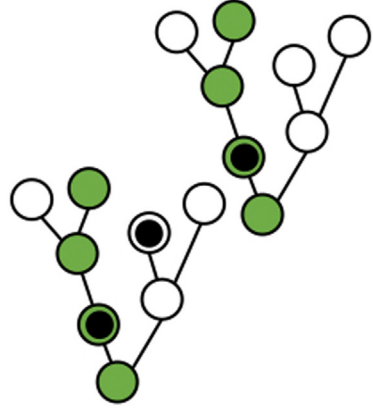
		Pathological staging	
		pN0	pN1+
Fluorescence Status	Patients with all their ICG-stained nodes negative for metastasis	Scenario 1  True-negative	Scenario 2  False-negative
		Scenario 3 Not possible (False-positive)	Scenario 4  True-positive

Fig. 1. Fluorescence status of lymph nodes identified in CaP patients by ICG-guided PLND and confirmatory ePLND.

Green circles represent LNs stained with ICG; white circles represent non-metastatic LNs not stained with ICG; black circles represent LNs with a pathological LNM; black circles superimposed onto green circles represent ICG-stained LNs with LNM; black circles superimposed onto white circles represent LNs with a LNM which are not ICG stained.

Scenario 1: patient with pN0 disease (no LNMs); **Scenario 2:** patient with pN1 disease but the LNM in the LN was not stained with ICG (false negative case); **Scenario 3:** is impossible in this context (because any ICG-LNM positive patients will always be pN1) but would otherwise correspond to false-positive cases in this confusion matrix; **Scenario 4:** patient with pN1 disease and at least one LNM stained with ICG.

Accuracy (Acc) refers to patients correctly classified by ICG-guided PLND either as disease positive or negative (true-positives and true-negatives, i.e. scenario 1 + scenario 4) from the sum of all the patients studied. **Sensitivity (Se)** refers to patients with ICG-guided PLND LNM-positive nodes divided by all the patients with positive lymph nodes (false-negative and true-positives, i.e., scenario 4 + scenario 2) and thus, quantifies the extent to which LNMs are not overlooked. **Negative predictive value (NPV)** refers to the probability that patients with no ICG-stained LNMs (true-positives, i.e., scenario 1) indeed do not have pN1 disease (false-negatives, i.e., scenario 2) and is calculated by dividing patients in scenario 1 by the sum of the patients in scenarios 1 and 2. **Negative test likelihood ratio [LR(-)]** refers to the probability that all the ICG-stained LNs in a person with pN1 disease are negative (false-negative) divided by the probability that all the ICG-stained LNs are negative in a pN0 patient (true-positive; i.e., scenario 2 divided by scenario 1); A ratio of less than 0.2 is usually indicative of the absence of disease.

Abbreviations are as follows: LN: lymph node; ICG: indocyanine green; pN: pathological nodal stage; LNM: lymph node metastasis; ICG-guided PLND: indocyanine green-guided lymphadenectomy; ePLND: extended pelvic lymph node dissection.

Table 1
Demographic, clinical, and pathological characteristics of the overall study cohort population stratified according to the EAU risk groups criteria

Variable	Intermediate-risk	High-risk	All patients	P-value
Patients, n. (%)	149 (68.0%)	70 (32.0%)	219 (100%)	
Age (years), median (IQR)	65 (59–70)	64 (60–69)	65 (59–69)	0.9
PSA (ng/ml), median (IQR)	6.1 (4.7–8.3)	9.0 (5.7–13.0)	6.8 (5.0–9.5)	< 0.001
BMI (kg/m ²), median (IQR)	27.5 (25.2–29.7)	26.5 (25.3–29.4)	27.2 (25.1–29.4)	0.42
Biopsy Gleason score, n. (%)				< 0.001
6	3 (2.0)	8 (11.0)	11 (5.0)	
7	146 (98.0)	33 (47.0)	179 (82.0)	
8–9	0 (0.0)	29 (41.0)	29 (13.0)	
Clinical Tumor stage, n. (%)				< 0.001
cT1	110 (73.8)	21 (30.0)	131 (59.8)	
cT2	39 (26.2)	15 (21.4)	54 (24.7)	
cT3	0 (0.0)	34 (48.6)	34 (15.5)	
Operative time (mins), median (IQR)	285 (240–300)	270 (240–300)	275 (240–300)	0.399
Number of ICG stained LNs, median (IQR)	6 (3–9)	6 (4–8)	6 (4–9)	0.664
Number of LNs removed, median (IQR)	21 (15–27)	22 (19–27)	22 (16–27)	0.123
pN1 disease, n. (%)	31 (20.8)	27 (38.6)	58 (26.5)	0.009
Number of LNMs, n. (%)				< 0.001
0	118 (79.2)	43 (61.4)	161 (73.5)	
1	22 (14.8)	8 (11.4)	30 (13.7)	
2	4 (2.7)	5 (7.1)	9 (4.1)	
3	3 (2.0)	3 (4.3)	6 (2.7)	
≥4	2 (1.4)	11 (15.7)	13 (6.1)	
Pathological Gleason score, n. (%)				< 0.001
6	11 (7.4)	3 (5.1)	14 (6.4)	
7	133 (89.3)	46 (78.0)	179 (81.7)	
8–10	5 (3.3)	10 (16.9)	26 (11.9)	
PSMs, n. (%)	30 (20.1)	23 (32.9)	53 (24.2)	0.06
Pathological Tumor stage, n. (%)				< 0.001
pT1–pT2	83 (55.7)	22 (31.4)	105 (47.9)	
pT3–pT4	66 (44.3)	48 (68.6)	114 (52.1)	
Follow-up (mos), median (IQR)	25.7 (14.7–36.4)	30.5 (19.1–41.0)	25.9 (16.2–36.9)	0.058

EAU= european association of urology; IQR= interquartile range; PSA= prostate specific antigen (levels before radical prostatectomy); BMI= body-mass index; ICG= indocyanine green; LN= lymph node; LNM= lymph node metastasis; pN= pathological nodal stage; PSMs= positive surgical margins; RP= radical prostatectomy.

vessels were successfully visualised by F-ICG-guided PLND in all the procedures. A median of 6 fluorescent LNs and a median of 22 (IQR 16–27) were per-patient dissected during the ePLND. Presence of LNMs (pN1) was reported in 58 (26%) cases. Of these, 30 (52%) patients had a single LNM. 26 (12%) patients had a pathological Gleason score ≥8, and 114 (52%) had pT3–pT4 disease (66 intermediate-risk and 48 high-risk). Positive surgical margins (PSMs) were reported in 53 (24%) patients.

3.3. Accuracy of F-ICG-guided PLND in the entire cohort

As mentioned, 58 patients had pN1 disease. In the per-patient analysis (Table 2), 53 individuals had one or more metastatic LNs among those stained with F-ICG (true-positive cases, scenario 4 in Fig. 1). In contrast, no LNs were stained with F-ICG in 5 pN1-patients (false negative cases, scenario 2 in Fig. 1). As shown in Table 3, the per-patient Acc of the F-ICG staining in

Table 2
Comparison of pN status by ICG-guided PLND versus ePLND at the 'per-patient' level.

	Intermediate-risk group		High-risk group		All patients	
	pN0	pN1	pN0	pN1	pN0	pN1
N. of patients with all ICG-stained nodes metastasis negative	118	3	43	2	161	5
N. of patients with any metastasis in ICG-stained nodes	0	28	0	25	0	53

The clinical classification of risk likelihood was performed according to the EAU risk groups criteria. Comparison of the true-positive and false-negative classification rates in patients in which all the ICG-stained LNs were metastasis-negative or metastasis-positive, respectively.

pN= pathological nodal status; ICG-guided PLND= indocyanine green-guided pelvic lymph node dissection; ePLND= extended pelvic lymph node dissection; ICG= indocyanine green; pN= pathological nodal stage.

Table 3

Diagnostic test results for the ‘per-patient’ evaluation of the reliability and specificity results for the presence of prostate cancer metastases detected by ICG-guided PLND versus ePLND

	Intermediate-risk group Estimation (95% CI)	High-risk group Estimation (95% CI)	All patients Estimation (95% CI)
ePLND Metastatic Prevalence	20.8 (14.6–28.2)	38.6 (27.2–51.0)	26.5 (20.8–32.9)
Accuracy	98.0 (94.2–99.7)	97.1 (90.1–99.7)	97.7 (94.8–99.3)
Sensitivity	90.3 (74.3–98.0)	92.6 (75.7–99.1)	91.4 (81.0–97.1)
NPV	97.5 (92.9–99.5)	95.6 (84.9–99.5)	97.0 (93.1–99.0)
Negative LR	9.7 (3.3–28.4)	7.4 (2.0–28.1)	8.6 (3.7–19.9)

ICG-guided PLND= indocyanine green-guided pelvic lymph node dissection; ePLND= extended pelvic lymph node dissection; ICG= indocyanine green; CI= confidence interval. NPV= Negative Predictive Value; LR= Likelihood Ratio.

Table 4

Outcomes reported as the number of lymph nodes: comparison of the identification of each single metastatic lymph node by ICG-guided PLND versus ePLND

	Intermediate-risk group			High-risk group			Overall		
	pN0	pN1	Total n. LNs	pN0	pN1	Total n. LNs	pN0	pN1	Total n. LNs
Non-ICG-stained nodes	2,110	12	2,122	1,072	51	1,123	3,182	63	3,245
ICG-stained nodes	1,019	39	1,058	407	70	477	1,426	109	1,535

ICG-guided PLND= indocyanine green-guided pelvic lymph node dissection; ePLND= extended pelvic lymph node dissection; ICG= indocyanine green; pN= pathological nodal stage.

the overall cohort was 97.7% (95%CI 94.8–99.3), NPV was 97.0% (95%CI 93.1–99.0), and LR(–) was 8.6% (95%CI 3.7–19.9). In terms of the per-node ability of F-ICG-guided PLND to identify LNMs, a total of 4780 nodes were removed and 1535 (32%) were intraoperatively fluorescent. Pathological evaluation (Table 4) revealed 172 (3.4%) metastatic LNMs, of which a total of 109 (63%) were ICG-stained. Among ICG-stained LNMs, 1426 LNMs were negative at final pathological report. As shown in Table 5, the per-node Acc of the F-ICG staining in the overall cohort was 68.9% (95%CI 67.5–70.2), NPV was 98.1% (95%CI 97.6–98.6), and LR(–) was 53.0% (95%CI 43.5–64.6).

3.4. Accuracy of F-ICG-guided PLND in intermediate-risk CaP patients

As shown in Table 2, in this subgroup, 31 patients were pN1. In the per-patient analysis, 28 patients had one or more metastatic LNMs among those stained with F-ICG (true-positive cases, scenario 4 in Fig. 1) while in 3 pN1-patients, all the stained nodes were disease-negative (false negative cases, scenario 2 in Fig. 1). As shown in Table 3, the per-patient Acc of the F-ICG staining in the intermediate-risk population was 98.0% (95%CI 94.2–99.7), NPV was 97.5% (95%CI 92.9–99.5), and LR(–) was 9.7% (95%CI 3.3–28.4). According to the per-node ability of F-

Table 5

Diagnostic test results for the evaluation of the ‘per-node’ reliability and specificity results for the presence of prostate cancer metastases detected by ICG-guided PLND versus ePLND

	Intermediate-risk group Estimation (95% CI)	High-risk group Estimation (95% CI)	All patients Estimation (95% CI)
ePLND Metastatic Prevalence	1.6 (1.2–2.1)	7.6 (6.3–9.0)	3.6 (3.1–4.2)
Accuracy	67.6 (65.9–69.2)	71.4 (69.1–73.6)	68.9 (67.5–70.2)
Sensitivity	76.5 (62.5–87.2)	57.9 (48.5–66.8)	63.5 (55.7–70.6)
NPV	99.4 (99.0–99.7)	95.5 (94.1–96.6)	98.1 (97.6–98.6)
Negative LR	34.9 (21.3–57.3)	58.2 (47.1–71.8)	53.0 (43.5–64.6)

ICG-guided PLND= indocyanine green-guided lymphadenectomy; ePLND= extended pelvic lymph node dissection; ICG= indocyanine green; NPV= Negative Predictive Value; LR= Likelihood Ratio; CI= confidence interval.

ICG-guided PLND to identify LNMs, a total of 3,180 nodes were removed in this subgroup and 1,058 (33%) were ICG-stained; pathological evaluation revealed 51 (1.6%) of these were metastatic LNMs; a total of 39 (76.5%) were ICG-stained. As shown in Table 5, the per-node Acc of the F-ICG staining in the intermediate-risk population was 67.6% (95%CI 65.9–69.2), NPV was 99.4% (95%CI 99.0–99.7), and LR(–) was 34.9% (95%CI 21.3–57.3).

3.5. Accuracy of F-ICG-guided PLND in high-risk CaP patients

A total of 27 (38.6%) high-risk patients were staged as pN1. In the per-patient analysis (Table 2), 25 individuals had one or more metastatic LNMs among those stained with F-ICG (true-positive cases, scenario 4 in Fig. 1) while all the stained nodes were disease-negative in 2 pN1-patients (false negative cases, scenario 2 in Fig. 1). As shown in Table 3, the per-patient Acc was 97.1% (95%CI 90.1–99.6), NPV was 95.6% (95%CI 84.9–99.5), and LR(–) was 7.4% (95%CI 2.0–28.1). Regarding the per-node analysis of the ability of F-ICG-guided PLND to identify LNMs (Table 4), a total of 1,600 nodes were removed from the high-risk subgroup and 477 (29.8%) of these were F-ICG-stained. The pathological report revealed the presence of 121 (7.6%) cancer-positive LNMs and 70 of these (57.9%) were F-ICG-stained LNMs. As shown in Table 5, the per-node Acc of the F-ICG staining in the high-risk cohort was 71.4% (95%CI 69.1–73.6), NPV was 95.5% (95%CI 94.1–96.6), and LR(–) was 58.2% (95%CI 47.1–71.8).

4. Discussion

In this prospective single-centre study we evaluated the ability of F-ICG to assess the LN status of patients who underwent laparoscopic RP and ePLND for clinical-localized CaP. We found that F-ICG-guided lymphangiography was a safe, cost-effective, and radiation-free procedure with no related adverse events. We observed a high per-patient NPV (97%) suggesting that avoiding ePLND would have been safe in the majority of patients when F-ICG-stained nodes were pN0. The per-patient LR(–) results were below 10%, indicating that F-ICG was able to discriminate between pN0 and pN1 CaP patients. However, the per-node sensitivity (63%) was insufficient to suggest that F-ICG could systematically replace ePLND.

Assessing LN status is a crucial step for tailoring treatments to individual patients. However, ePLND can cause significant morbidity exposing patients to perioperative risks [7]. To avoid these complications, a targeted SN dissection technique was proposed [9,11]. Vit et al. showed that the pooled diagnostic accuracy of different SN procedures was comparable to ePLND with an overall median Se and NPV of 95.2% and 98.0%, respectively [14]. In our cohort, 58 (26.5%) patients had LNMs, a finding slightly

higher than the range found in similar ICG-guided series (8%–20%) [9,12,18] which might be due to the higher incidence of locally-advanced disease in our cohort. Only one randomized prospective trial has so far evaluated the role of F-ICG-guided procedure in CaP [18]. This trial included a total of 59 patients and observed a Se of 78%, a finding which could perhaps be partially explained by the smaller sample size and the lower rate of pN1 (12.7%) patients these authors reported [18]. In our experience, an increased prevalence of LNMs might have influenced the NPV. However, the fact the NPV in our study still remained as high as 97% supports the idea that, as a rule of thumb, if stained LNMs are negative, no nodes will be positive in the later pathological analysis.

Controversy exists regarding the adoption of SN procedures in CaP. These include the multifocality of CaP that makes challenging a precise peritumoral tracer injection, different approaches (transrectal vs. transperineal), and the lack of a single SN within a complex lymphatic drainage system [14]. Thus, different primary tumour sites within the prostate gland may have different lymphatic dissemination patterns [19]. Several techniques and sites of tracers' deposition have been described. Korne et al. performed a transrectal injection of ICG-^{99m}Tc-nanocolloid in the peripheral zone. Accordingly, the authors further divided the prostate into four quadrants considering 3 different orientations: left vs. right, dorsal vs. ventral, and base vs. apex. A median of 4.3 sentinel LNMs per patients were found within a cohort of 67 patients [20]. Miki et al. injected F-ICG into the peripheral zone of bilateral lobes through a transrectal approach showing a median of 4 sentinel LNMs per patient in a prospective cohort of 50 individuals [21]. We transperineally injected F-ICG in the middle of the transitional zone of each prostatic lobe describing a median of 6 fluorescent LNMs for each patient. In this context, MRI-guided ultrasound-fusion needle navigation technologies have the potential to allow precise targeting of multiple CaP sites described at time of prostate biopsy [22].

The most important drawback of SN procedures in CaP is the lack of reliable techniques for intraoperative SN analysis. Here, Winter et al. reported the first results about one-step-nucleic-acid-amplification (OSNA) in CaP quantifying the CK19-mRNA copies. OSNA was performed on frozen samples using a ready-to-use amplification kit in an automated real-time detection system and compared with standard histopathological and immunohistochemical examinations. With a CK19-mRNA copy number cut-off of 250 copies/ μ l the authors showed promising results in order to improve intraoperative LN assessment [23]. Importantly, the availability of fast and reliable intraoperative analysis techniques for F-ICG-stained nodes would help surgeons to make intraoperative decisions about whether to proceed or abort ePLND. Given that we obtained a NPV of 97%, ePLND could have been avoided in 3 out of 4 of the patients we studied with fewer than 3% of these individuals having been misclassified. Furthermore, given the strong

association found between the LNs identified with F-ICG and radioisotope ^{99m}Tc -SN dissection, it is likely that fluorescence- will eventually replace classic radio-guided SN procedure [10].

As proposed by the Sentinel Node Prostate Cancer Consensus Panel Group, a meticulous histological processing of the fluorescent LNs was applied to exclude the presence of micrometastases [24]. Based on well-established breast cancer SN protocols, we analyzed 250- μm thick LN slides [25]. Given that about 80% of metastatic LNs in CaP are smaller than 8 mm [26], the Se of morphological cross-sectional imaging remains low [15]. To overcome these limitations, positron-emission tomography CT (PET-CT) combined with ^{68}Ga - or ^{18}F -labelled prostate specific membrane antigen (PSMA) appears to outperform traditional imaging modalities [27]. A recent systematic review comprising a total of 1,597 patients with intermediate- or high-risk CaP prior to RP demonstrated a pooled Se of 65% (95%CI 49–79) for ^{68}Ga -PSMA PET-CT suggesting that this modality may impact clinical decision making [28]. Incorporating these preoperative PSMA findings with our intraoperative F-ICG at the per-patient level prompt that the use of these two techniques need not be mutually exclusive and indeed, they could be complementary to each other. Thus, developing a hybrid tracer might be advantageous in the diagnosis and staging of CaP. In fact, previous authors were already able to integrate PSMA-targeted surgery both in an open [29] and robot-assisted setting [30].

The current report had some limitations. First, there is no clear consensus on the ideal F-ICG dilution for this application and no well-designed phase I dose escalation trials have been yet carried out. Second, fluorescence imaging has limited tissue penetration. Third, F-ICG continues to be shown up to 3 hours after intraprostatic injection. The strengths of this study were its prospective design, well-standardised F-ICG-guided PLND and ePLND procedures, homogeneity in treatment allocation regarding the intraprostatic tracer injection, a meticulous and therefore representative PLND, strict pathological evaluation, and implementation by 3 different surgeons. Although our experience focused on laparoscopic RP, current da Vinci robotic platforms are now equipped with a Firefly fluorescence laparoscope designed to support white light imaging as well as the detection of F-ICG. To the best of our knowledge, this data represents the largest prospective series on F-ICG-guided PLND published in the literature to date.

5. Conclusions

F-ICG guided-PLND before RP is a feasible and reliable method for LN status evaluation in CaP patients. Here, F-ICG-guided PLND correctly staged CaP in almost 98% of the patients in our cohort. However, the reduced Se of per-node F-ICG means that ePLND cannot be systematically avoided. Nonetheless, the high per-patient NPV we observed for F-ICG guided-PLND could allow surgeons to

avoid ePLND during RP in CaP patients when intraoperative fluorescent LN analysis is available.

Ethics approval and consent to participate

This prospective study was performed in accordance with the Declaration of Helsinki and was approved by the central ethics committee (Institutional Review Board approval CaPROS-IVO) at Fundaci3n Insituto Valenciano de Oncologia. Written informed consent was obtained from all the participants.

Conflict of interest

The authors declare that there are no conflict of interest.

Acknowledgments

None.

References

- [1] Siegel RL, Miller KD, Jemal A. Cancer statistics, 2020. *CA Cancer J Clin* 2020;70:7–30. <https://doi.org/10.3322/caac.21590>.
- [2] Briganti A, Larcher A, Abdollah F, Capitanio U, Gallina A, Suardi N, et al. Updated nomogram predicting lymph node invasion in patients with prostate cancer undergoing extended pelvic lymph node dissection: the essential importance of percentage of positive cores. *Eur Urol* 2012;61:480–7. <https://doi.org/10.1016/j.eururo.2011.10.044>.
- [3] Briganti A, Chun FKH, Salonia A, Zanni G, Scattoni V, Valiquette L, et al. Validation of a nomogram predicting the probability of lymph node invasion among patients undergoing radical prostatectomy and an extended pelvic lymphadenectomy. *Eur Urol* 2006;49:1019–27. <https://doi.org/10.1016/j.eururo.2006.01.043>.
- [4] Gandaglia G, Ploussard G, Valerio M, Mattei A, Fiori C, Fossati N, et al. A novel nomogram to identify candidates for extended pelvic lymph node dissection among patients with clinically localized prostate cancer diagnosed with magnetic resonance imaging-targeted and systematic biopsies. *Eur Urol* 2019;75:506–14. <https://doi.org/10.1016/j.eururo.2018.10.012>.
- [5] Briganti A, Blute ML, Eastham JH, Graefen M, Heidenreich A, Karnes JR, et al. Pelvic lymph node dissection in prostate cancer. *Eur Urol* 2009;55:1251–65. <https://doi.org/10.1016/j.eururo.2009.03.012>.
- [6] Van Den Bergh L, Lerut E, Haustermans K, Deroose CM, Oyen R, Isebaert S, et al. Final analysis of a prospective trial on functional imaging for nodal staging in patients with prostate cancer at high risk for lymph node involvement. *Urol Oncol Semin Orig Investig* 2015;33:109.e23–31. <https://doi.org/10.1016/j.urolonc.2014.11.008>.
- [7] Fossati N, Willemsse PPM, Van den Broeck T, van den Bergh RCN, Yuan CY, Briers E, et al. The benefits and harms of different extents of lymph node dissection during radical prostatectomy for prostate cancer: a systematic review. *Eur Urol* 2017;72:84–109. <https://doi.org/10.1016/j.eururo.2016.12.003>.
- [8] van Leeuwen FWB, Winter A, van Der Poel HG, Eiber M, Suardi N, Graefen M, et al. Technologies for image-guided surgery for managing lymphatic metastases in prostate cancer. *Nat Rev Urol* 2019;16:159–71. <https://doi.org/10.1038/s41585-018-0140-8>.
- [9] Manny TB, Patel M, Hemal AK. Fluorescence-enhanced robotic radical prostatectomy using real-time lymphangiography and tissue marking with percutaneous injection of unconjugated indocyanine green: the initial clinical experience in 50 patients. *Eur Urol* 2014;65:1162–8. <https://doi.org/10.1016/j.eururo.2013.11.017>.

- [10] Jeschke S, Lusuardi L, Myatt A, Hraby S, Pirich C, Janetschek G. Visualisation of the lymph node pathway in real time by laparoscopic radioisotope- and fluorescence-guided sentinel lymph node dissection in prostate cancer staging. *Urology* 2012;80:1080–7. <https://doi.org/10.1016/j.urology.2012.05.050>.
- [11] Ramírez-Backhaus M, Mira Moreno A, Gómez Ferrer A, Calatrava Fons A, Casanova J, Solsona Narbón E, et al. Indocyanine green guided pelvic lymph node dissection: an efficient technique to classify the lymph node status of patients with prostate cancer who underwent radical prostatectomy. *J Urol* 2016;196:1429–35. <https://doi.org/10.1016/j.juro.2016.05.087>.
- [12] Yuen K, Miura T, Sakai I, Kiyosue A, Yamashita M. Intraoperative fluorescence imaging for detection of sentinel lymph nodes and lymphatic vessels during open prostatectomy using indocyanine green. *J Urol* 2015;194:371–7. <https://doi.org/10.1016/j.juro.2015.01.008>.
- [13] Cacciamani GE, Shakir A, Tafuri A, Gill K, Han J, Ahmadi N, et al. Best practices in near-infrared fluorescence imaging with indocyanine green (NIRF/ICG)-guided robotic urologic surgery: a systematic review-based expert consensus. *World J Urol* 2020;38:883–96. <https://doi.org/10.1007/s00345-019-02870-z>.
- [14] Wit EMK, Acar C, Grivas N, Yuan C, Horenblas S, Liedberg F, et al. Sentinel node procedure in prostate cancer: a systematic review to assess diagnostic accuracy. *Eur Urol* 2017;71:596–605. <https://doi.org/10.1016/j.eururo.2016.09.007>.
- [15] Mottet van den B N, Briers PCE, De Santis M, Fanti S, Gillessen S, Grummet AMH J, et al. EAU - EANM - ESTRO - ESUR - SIOG Guidelines on Prostate Cancer 2019. *Eur Assoc Urol Guidel* 2019;53:1–161.2019.
- [16] Claps F, Ramírez-Backhaus M, Mire Maresma MC, Gómez-Ferrer Á, Mascarós JM, Marengo J, et al. Indocyanine green guidance improves the efficiency of extended pelvic lymph node dissection during laparoscopic radical prostatectomy. *Int J Urol* 2021;28. <https://doi.org/10.1111/iju.14513>.
- [17] Assel M, Sjoberg D, Elders A, Wang X, Huo D, Botchway A, et al. Guidelines for reporting of statistics for clinical research in urology. *Eur Urol* 2019;75:358–67. <https://doi.org/10.1016/j.eururo.2018.12.014>.
- [18] Harke NN, Godes M, Wagner C, Addali M, Fangmeyer B, Urbanova K, et al. Fluorescence-supported lymphography and extended pelvic lymph node dissection in robot-assisted radical prostatectomy: a prospective, randomized trial. *World J Urol* 2018;36:1817–23. <https://doi.org/10.1007/s00345-018-2330-7>.
- [19] Løvf M, Zhao S, Axcrona U, Johannessen B, Bakken AC, Carm KT, et al. Multifocal primary prostate cancer exhibits high degree of genomic heterogeneity. *Eur Urol* 2019;75:498–505. <https://doi.org/10.1016/j.eururo.2018.08.009>.
- [20] de Korne CM, Wit EM, de Jong J, Valdés Olmos RA, Buckle T, van Leeuwen FWB, et al. Anatomical localization of radiocolloid tracer deposition affects outcome of sentinel node procedures in prostate cancer. *Eur J Nucl Med Mol Imaging* 2019;46:2558–68. <https://doi.org/10.1007/s00259-019-04443-z>.
- [21] Miki J, Yanagisawa T, Tsuzuki S, Mori K, Urabe F, Kayano S, et al. Anatomical localization and clinical impact of sentinel lymph nodes based on patterns of pelvic lymphatic drainage in clinically localized prostate cancer. *Prostate* 2018;78:419–25. <https://doi.org/10.1002/pros.23486>.
- [22] Van Oosterom MN, Van Der Poel HG, Navab N, Van De Velde CJH, Van Leeuwen FWB. Computer-assisted surgery: virtual- and augmented-reality displays for navigation during urological interventions. *Curr Opin Urol* 2018;28:205–13. <https://doi.org/10.1097/MOU.0000000000000478>.
- [23] Winter A, Engels S, Goos P, Süykens MC, Henke RP, Gerullis H, et al. Detection of ck19 mRNA using one-step nucleic acid amplification (OSNA) in prostate cancer: preliminary results. *J Cancer* 2018;9:4611–7. <https://doi.org/10.7150/jca.26794>.
- [24] van der Poel HG, Wit EM, Acar C, van den Berg NS, van Leeuwen FWB, Valdes Olmos RA, et al. Sentinel node biopsy for prostate cancer: report from a consensus panel meeting. *BJU Int* 2017;120:204–11. <https://doi.org/10.1111/bju.13810>.
- [25] Manca G, Tardelli E, Rubello D, Gennaro M, Marzola MC, Cook GJ, et al. Sentinel lymph node biopsy in breast cancer: a technical and clinical appraisal. *Nucl Med Commun* 2016;37:570–6. <https://doi.org/10.1097/MNM.0000000000000489>.
- [26] Heesakkers RA, Hövels AM, Jager GJ, van den Bosch HC, Witjes JA, Raaij HP, et al. MRI with a lymph-node-specific contrast agent as an alternative to CT scan and lymph-node dissection in patients with prostate cancer: a prospective multicohort study. *Lancet Oncol* 2008;9:850–6. [https://doi.org/10.1016/S1470-2045\(08\)70203-1](https://doi.org/10.1016/S1470-2045(08)70203-1).
- [27] Corfield J, Perera M, Bolton D, Lawrentschuk N. 68Ga-prostate specific membrane antigen (PSMA) positron emission tomography (PET) for primary staging of high-risk prostate cancer: a systematic review. *World J Urol* 2018;36:519–27. <https://doi.org/10.1007/s00345-018-2182-1>.
- [28] Wu H, Xu T, Wang X, Yu YB, Fan ZY, Li DX, et al. Diagnostic performance of 68gallium labelled prostate-specific membrane antigen positron emission tomography/computed tomography and magnetic resonance imaging for staging the prostate cancer with intermediate or high risk prior to radical prostatectomy: a systematic review and meta-analysis. *World J Mens Health* 2020;38:208–19. <https://doi.org/10.5534/wjmh.180124>.
- [29] Maurer T, Robu S, Schottelius M, Schwamborn K, Rauscher I, van den Berg NS, et al. 99m technetium-based prostate-specific membrane antigen–radioguided surgery in recurrent prostate cancer. *Eur Urol* 2019;75:659–66. <https://doi.org/10.1016/j.eururo.2018.03.013>.
- [30] Van Leeuwen FWB, Van Oosterom MN, Meershoek P, Van Leeuwen PJ, Berliner C, Van Der Poel HG, et al. Minimal-invasive robot-assisted image-guided resection of prostate-specific membrane antigen-positive lymph nodes in recurrent prostate cancer. *Clin Nucl Med* 2019;44:580–1. <https://doi.org/10.1097/RLU.0000000000002600>.